Energy level engineering in ternary organic solar cells: Evaluating exciton dissociation at organic semiconductor interfaces

Krishna Feron, Mahir N. Thameel, Mohammed F. Al-Mudhaffer, Xiaojing Zhou, Warwick J. Belcher, Christopher J. Fell, and Paul C. Dastoor

Citation: Appl. Phys. Lett. **110**, 133301 (2017); doi: 10.1063/1.4979181
View online: http://dx.doi.org/10.1063/1.4979181
View Table of Contents: http://aip.scitation.org/toc/apl/110/13
Published by the American Institute of Physics

Energy level engineering in ternary organic solar cells: Evaluating exciton dissociation at organic semiconductor interfaces

Krishna Feron,[1,2,a)] Mahir N. Thameel,[2,3] Mohammed F. Al-Mudhaffer,[2,4] Xiaojing Zhou,[2] Warwick J. Belcher,[2] Christopher J. Fell,[1] and Paul C. Dastoor[2]
[1]*CSIRO Energy, Newcastle, NSW 2300, Australia*
[2]*Centre for Organic Electronics, University of Newcastle, University Drive, Callaghan, NSW 2308, Australia*
[3]*Department of Physics, College of Education for pure science, University of Anbar, Ramadi, Anbar 31001, Iraq*
[4]*Department of Physics, College of Education for Pure Science, University of Basrah, Basrah 61004, Iraq*

(Received 13 September 2016; accepted 14 March 2017; published online 27 March 2017)

Electronic energy level engineering, with the aim to improve the power conversion efficiency in ternary organic solar cells, is a complex problem since multiple charge transfer steps and exciton dissociation driving forces must be considered. Here, we examine exciton dissociation in the ternary system poly(3-hexylthiophene): [6,6]-phenyl-C61-butyric acid methyl ester:2,4-bis[4-(N,N-diisobutylamino)-2,6-dihydroxyphenyl] squaraine (P3HT:PCBM:DIBSq). Even though the energy level diagram suggests that exciton dissociation at the P3HT:DIBSq interface should be efficient, electron paramagnetic resonance and external quantum efficiency measurements of planar devices show that this interface is not capable of generating separated charge carriers. Efficient exciton dissociation is still realised via energy transfer, which transports excitons from the P3HT:DIBSq interface to the DIBSq:PCBM interface, where separated charge carriers can be generated efficiently. This work demonstrates that energy level diagrams alone cannot be relied upon to predict the exciton dissociation and charge separation capability of an organic semiconductor interface and that energy transfer relaxes the energy level constraints for optimised multi-component organic solar cells. *Published by AIP Publishing.* [http://dx.doi.org/10.1063/1.4979181]

The photoactive layer in organic solar cells has seen a progression from unary to binary[1] material systems to improve exciton dissociation.[2] More recently, ternary organic solar cells are fabricated and in many cases exhibit improved performance over their binary equivalents.[3] An example of a ternary system[4] is poly(3-hexylthiophene): [6,6]-phenyl-C61-butyric acid methyl ester:2,4-bis[4-(N,N-diisobutylamino)-2,6-dihydroxyphenyl] squaraine (P3HT:PCBM:DIBSq), which is the focus of this study.

Ternary systems are more complex than binary systems in regard to understanding the photoconversion mechanism, since they require controlling the mesoscopic structure and identifying materials with complementary electronic energy levels to yield high power conversion efficiency (PCE). For efficient charge transfer between the three semiconductors, a cascade energy level system is required, as shown in Figure 1. Such a cascade structure not only allows for thermodynamically favourable charge carrier transport, but the large energy offsets also ensure that excitons are able to dissociate at each interface. In particular, the energy offsets at each interface must be larger than the exciton binding energy to efficiently dissociate excitons,[2] which results in a considerable energy loss. Exciton binding energies are reported to range from 0.3 to 0.6 eV.[5] However, since the binding energy differs between materials due to, for example, the exciton delocalisation in each material, the precise magnitude of the energy offset required at each interface is unclear.

A blend of three semiconductors gives rise to three interfaces: in this case, P3HT:PCBM, P3HT:DIBSq and PCBM:DIBSq. Since exciton dissociation at each interface may occur via hole transfer or electron transfer, excitons in a ternary blend may dissociate through one of six different charge transfer steps with rates that are determined by the associated energy offset. Each of these energy offsets is designated as shown in Figure 1 where the energy offsets were determined using photoelectron spectroscopy in air (PESA) and absorption spectroscopy.[6]

Energy diagrams like the one presented in Figure 1 are commonly used to predict whether a ternary material system will dissociate excitons efficiently and generate separated

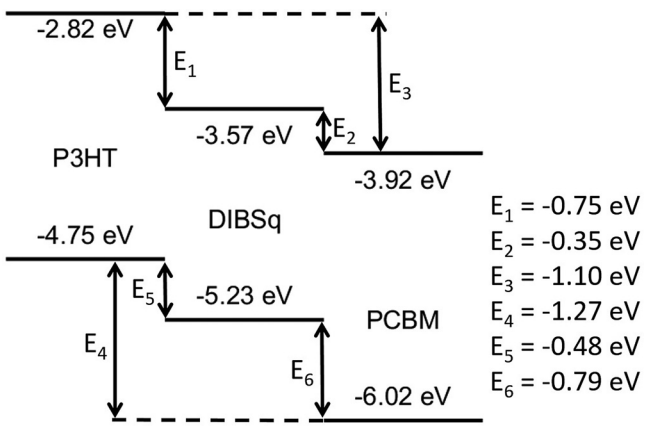

FIG. 1. Energy level diagram for P3HT:PCBM:DIBSq. Using PESA, the HOMO was measured to be −4.75 eV, −5.23 eV and −6.02 eV for P3HT, DIBSq and PCBM, respectively. The optical band gap was added to the HOMO to obtain the LUMO at −2.82, −3.57 and −3.92 eV for P3HT, DIBSq and PCBM, respectively.

a)Electronic mail: Krishna.Feron@csiro.au

charge carriers.[7–9] Assuming that the exciton binding energy is 0.3 eV,[9] the driving energy for charge transfer across the interface is estimated to be larger than the exciton binding energy in all six cases, meaning that one might expect efficient exciton dissociation at any interface in a P3HT:PCBM:DIBSq system. Furthermore, the measured external quantum efficiency suggests that P3HT:PCBM:DIBSq devices are efficient across the entire spectral absorption range of the device,[4] indicating that all three photoactive components are absorbing light and giving rise to charge carriers. Hence, it appears to be a valid assumption that the six different energy offsets (losses) shown in Figure 1 are contributing toward exciton dissociation and thus serving a purpose in the photovoltaic device. However, it has also been shown that hetero energy transfer is prevalent in P3HT:PCBM:DIBSq devices,[4] i.e., excitons absorbed in one species move to another species and dissociate at an unexpected interface.[6] As such, the favourability for dissociation at any particular interface is unclear. Since each dissociation comes with an energy loss that reduces the maximum attainable open-circuit voltage (V_{OC}), it is useful to know which energy offsets could be decreased without affecting the overall exciton dissociation efficiency.

In order to address this problem, exciton dissociation at the P3HT:DIBSq interface was investigated using electron paramagnetic resonance (EPR) measurements. EPR detects unpaired electrons, such as polarons, which can be either intrinsic to the material or generated by photoexcitation. EPR experiments were conducted using a Bruker EMXplus. Illumination of the EPR samples was achieved using a 250 W Halogen lamp positioned approximately 30 cm away from the sample compartment. The cavity is flooded with cooled gaseous nitrogen to avoid further photoinduced oxidation during the measurement and to provide temperature control. Chlorobenzene solutions of P3HT:PCBM (1:0.8 wt. %), P3HT:DIBSq (1:0.05 wt. %), P3HT:PCBM:DIBSq(1:0.8:0.05 wt. %), P3HT:PCBM:DIBSq (1:0.8:0.025 wt. %) and P3HT were drop cast on plastic substrates (cellulose acetate). The substrates were cut to size (approximately 4 mm wide and 2 cm long), inserted in the sample tube and cooled using liquid nitrogen. Low temperatures are required to improve the signal-to-noise ratio for this measurement; however, the results must still be applicable to the device working conditions, i.e., at room temperature. It is known that the photovoltaic behaviour changes at temperatures below 150 K; for example, the V_{OC} exhibits nonlinear behaviour[10] and the fluorescence quantum efficiency[11] (and thus the energy transfer rate) and exciton diffusion coefficients[12,13] change as well. Since energy transfer from P3HT to DIBSq is efficient in P3HT:PCBM:DIBSq systems, both direct and two-step exciton dissociation mechanisms are expected to occur.[6] The prevalence of these two dissociation modes could change depending on temperature due to a change in the exciton hopping and energy transfer rates. Consequently, the exciton dissociation mechanism and thus charge generation efficiency could change when lowering the temperature <150 K. In order to maximise the signal-to-noise whilst avoiding changes in the photoconversion mechanism, the EPR measurements were conducted at 200 K. At higher temperatures, polarons could not be adequately detected. The EPR spectrum for a P3HT film is shown in Figure 2(a). A Landé g-factor of 2.003 was observed, which corresponds to a positive polaron (P^+) on the P3HT backbone.[14] EPR measurements were performed in the dark as well as with light provided by a halogen lamp. It is known that P3HT becomes doped when exposed to air,[15] giving rise to an intrinsic polaron population that is unaffected by light exposure.[14] Light does not change the P^+ population in the P3HT film due to the lack of a heterointerface, where excitons can dissociate efficiently and thus only the intrinsic EPR response is measured. By contrast, the P3HT:PCBM interface has large associated energy offsets (E_3 and E_4 in Figure 1) and dissociates excitons efficiently, producing charge-separated states at the heterointerfaces that are readily detected by the EPR measurement. Consequently, the P3HT:PCBM film does exhibit an increase in the P^+ population when exposed to light (Figure 2(b)). The paramagnetic susceptibility of the PCBM and bisPCBM polarons (P^-) decreases much more rapidly with increasing temperature than that of P^+.[16,17] Hence, P^- is not seen in the EPR spectrum measured at 200 K. Measurements were also conducted at 170 K where the characteristic EPR signature of P^- is noticeable (see supplementary material). Due to the low paramagnetic susceptibility of P^- at 200 K, P^+ is a better proxy for the photogenerated charge carriers.

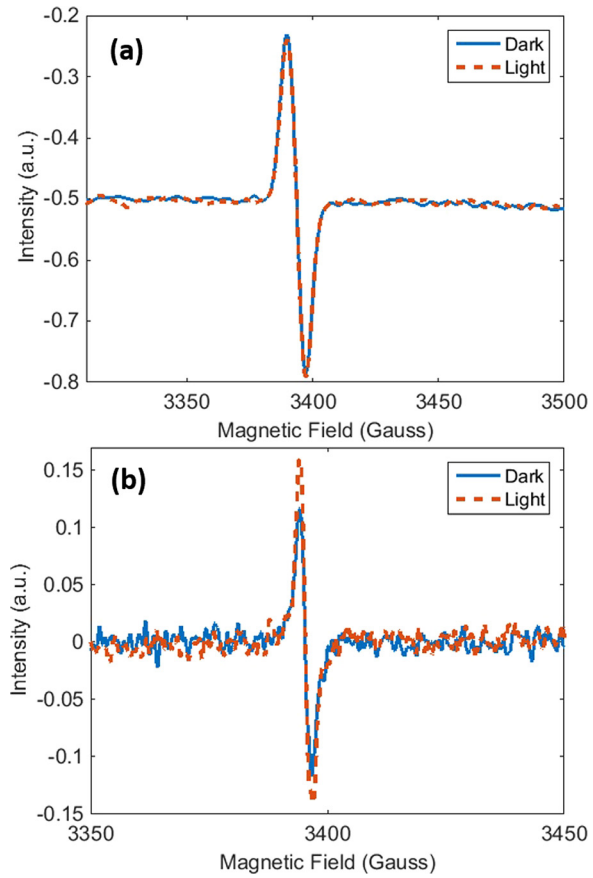

FIG. 2. (a) EPR spectra of a P3HT film with and without illumination. (b) EPR spectra of a P3HT:PCBM film with and without illumination.

The P+ population increase due to light exposure was quantified by calculating the area under the cumulative integrated EPR absorption curves (see supplementary material) for the films of P3HT, P3HT:DIBSq (1:0.05 wt. ratio), P3HT:PCBM (1:0.8 wt. ratio), P3HT:PCBM:DIBSq (1:0.8:0.025 wt. ratio) and P3HT:PCBM:DIBSq (1:0.8:0.05 wt. ratio), and these values are plotted in Figure 3. The thickness of the films ranged from 7.5 μm to 8 μm, which is larger than the optical

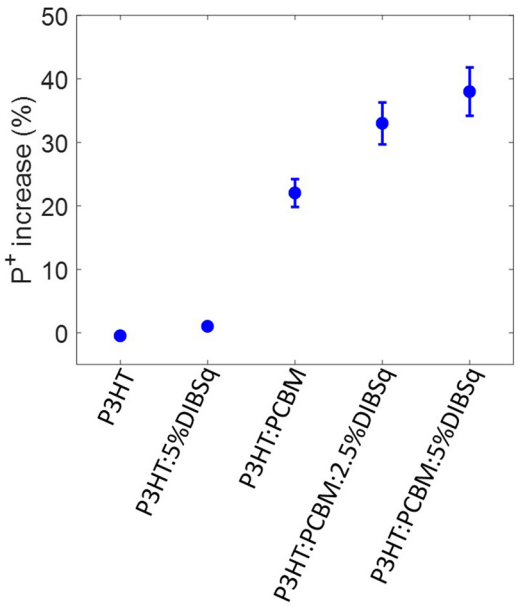

FIG. 3. The P+ population increase upon light exposure for various combinations of P3HT, PCBM and DIBSq films. Error bars are based on the estimated variation in the optically accessible and inaccessible semiconductor volumes across the samples.

penetration depth. However, the films only varied in thickness by less than 7%, and the extinction coefficient is approximately the same for all samples meaning that the optically accessible and inaccessible semiconductor volumes are estimated to be the same for all samples to within 10%. Hence, the observed increase in P+ population upon light exposure gives a semi-quantitative measure of the relative amount of photogenerated charge. The observed increase in P+ population upon light exposure is above the observed noise in the measurement results and is repeatable. The same trend is seen when measurements are conducted at 170 K (see supplementary material). The P+ population does not increase upon light exposure for the P3HT and P3HT:DIBSq films. P3HT:PCBM and P3HT:PCBM:DIBSq films, on the other hand, do show a substantial increase in the P+ population upon illumination. These results can be explained by the following one of the two mechanisms:

(1) The P3HT:PCBM interface generates charge carriers, while the P3HT:DIBSq does not.
(2) Continuous wave EPR measurements are more sensitive to long-lived charge carriers. In addition to the P3HT:PCBM interface, the P3HT:DIBSq interface also generates charge carriers. However, the P+ population at the P3HT:DIBSq interface has very short lifetimes compared to the P+ population at the P3HT:PCBM interface and is not seen in the EPR measurements.

If the P3HT:DIBSq interface would inherently generate P+ polarons with a significantly shorter lifetime to the P+ polarons generated at a P3HT:PCBM interface, the P3HT:DIBSq is likely to act as a site for recombination. However, the addition of DIBSq to the P3HT:PCBM blend is seen to increase the photocurrent, fill factor and power conversion efficiency.[4] Furthermore, DIBSq has been used in various efficient binary photovoltaic systems.[18,19] In other words, DIBSq is unlikely to introduce recombination sites in P3HT:fullerene devices, which makes scenario #2 improbable. As such, the EPR measurements suggest that excitons do not dissociate efficiently at the P3HT:DIBSq interface. Furthermore, the P+ population is observed to increase with DIBSq concentration, which not only indicates that exciton dissociation is more efficient in the ternary films, but that charge generation is also improved. More efficient dissociation with the addition of DIBSq is indeed predicted by kinetic Monte Carlo modelling of exciton transport and is ascribed to long-range energy transfer from P3HT to DIBSq.[6] Despite the large energy offsets at the P3HT:DIBSq interface (E_1 and E_5 in Figure 1), the EPR results associated with the P3HT:DIBSq sample did not show evidence for exciton dissociation, meaning that excitons only dissociate at the P3HT:PCBM interface and potentially at the DIBSq:PCBM interface.

To further test this hypothesis, a series of planar photovoltaic devices were fabricated from P3HT:DIBSq, P3HT:C60, DIBSq:C60 and P3HT:DIBSq:C60. All devices had the same anode and cathode, which were ITO-PEDOT:PSS and Bathocuproine-Aluminium, respectively. All layers were thermally deposited except the PEDOT:PSS and P3HT layers, which were deposited via spin-coating. The device structures of these solar cells are shown in the supplementary material. The devices were not annealed, so as to prevent intermixing of the stacked layers. All devices showed a photovoltaic response, except for the P3HT:DIBSq device, which again suggests that the P3HT:DIBSq interface does not dissociate excitons. The absorption spectra for the three individual materials, along with the device structures, are included in the supplementary material. Each material has distinct absorption peaks: C_{60} has a peak at 420 nm, P3HT at 555 nm and 600 nm, and DIBSq at 680 nm. These distinct peaks allow us to estimate the contribution of each individual material to the external quantum efficiency (EQE) of the devices. Optical constants were estimated from absorption spectra of individual layers on quartz substrates using a methodology discussed previously[20] and in the supplementary information. The optical constants were subsequently used to model the light absorption in each layer/material for the series of planar device structures using the transfer matrix method. It is assumed that the incident light propagates in one dimension through the device layers and the layers are homogeneous and isotopic and have parallel, flat interfaces. The negative derivative of the Poynting vector was used to estimate the absorbance spectrum. The contribution of each material to the *EQE* was determined by fitting the following equation to the experimentally measured *EQE*.

$$EQE = IQE^{P3HT} \cdot A^{P3HT} + IQE^{DIBSq} \cdot A^{DIBSq} + IQE^{C_{60}} \cdot A^{C_{60}} \quad (1)$$

IQE is the internal quantum efficiency and *A* is the fraction of absorbed light. Superscripts denote the 3 materials. The orthogonality of the three absorption spectra ensures that a unique single solution exists for this minimisation problem. The *IQE* for each material in each device structure is shown in Table I and associated fits are shown in Figure 4. The *EQE* fits are good where P3HT and C_{60} absorb light. The *EQE* peak at 680 nm, associated with DIBSq, is not exactly reproduced by the optical model. The modelled absorption at

TABLE I. *IQE* for P3HT, DIBSq and C60 in the 4 fabricated device structures.

Device structure	IQE^{P3HT} (%)	IQE^{DIBSq} (%)	IQE^{C60} (%)
P3HT(40 nm):C_{60}(50 nm)	5.53	…	12.5
P3HT(40 nm):DIBSq (14 nm)	0	0	…
DIBSq(14 nm):C_{60}(50 nm)	…	42.7	22.4
P3HT(40 nm):DIBSq(14 nm):C_{60}(50 nm)	0	20.1	11.6

680 nm is broader and slightly red-shifted compared to the associated peak seen in the *EQE* spectrum.

It is well known that DIBSq forms J-aggregates,[21] which causes broadening and red-shifting of the absorption spectrum,[18] and that the aggregation behaviour is sensitive to processing/fabrication conditions.[18] The complex dielectric function of DIBSq was determined using thicker, solid DIBSq films on quartz, while the DIBSq film in a device stack is thinner and sandwiched between either P3HT and C_{60} or PEDOT:PSS and C_{60}. As such, different degrees/types of aggregation are expected for DIBSq on quartz, resulting in a broadened and red-shifted absorption spectrum compared to DIBSq in a device stack. Regardless of the quality of fit in the DIBSq wavelength region, it is clear that P3HT does not contribute to photocurrent when not in contact with C_{60}, even though P3HT is the main light absorber (Fig. S3, supplementary material). Both the ternary and the P3HT:DIBSq binary devices show no photocurrent contribution from P3HT, corroborating the hypothesis that the P3HT:DIBSq interface does not dissociate excitons. Since DIBSq and C_{60} both contribute to photocurrent in the ternary device, the DIBSq:C_{60} interface must be capable of dissociating excitons and P3HT must be able to conduct charge carriers. So, while the energetic driving force at the P3HT:DIBSq interface is not sufficiently large to split excitons, it is certainly large enough to facilitate charge transfer.

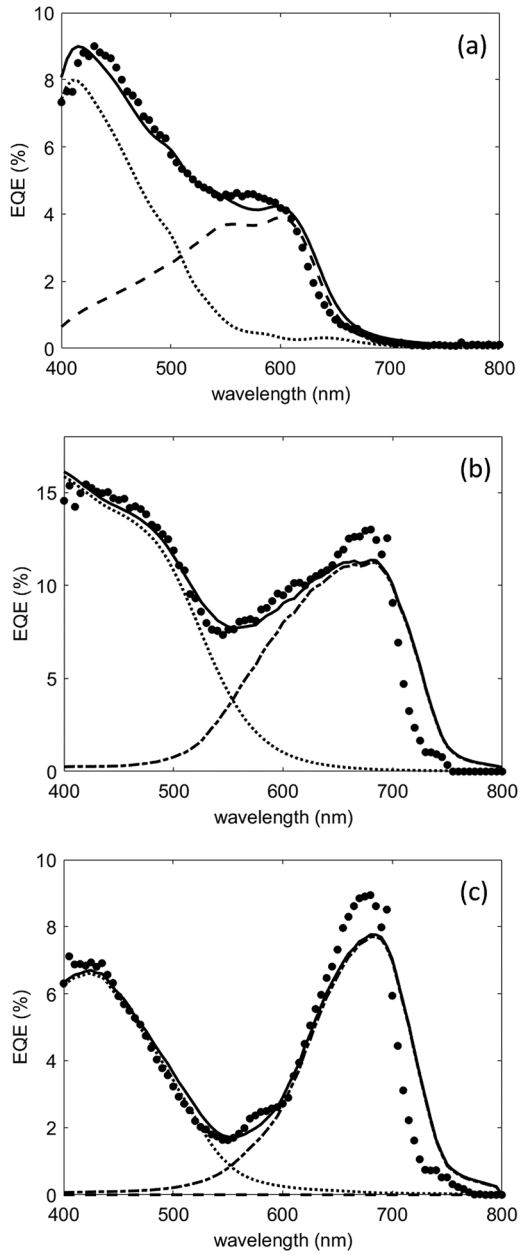

FIG. 4. Measured *EQE* spectra (dots), *EQE* spectra fit (solid), C_{60} contribution (short dashes), P3HT contribution (long dashes) and DIBSq contribution (short dash-long dash) are shown for (a) P3HT:C_{60}, (b) DIBSq:C_{60} and (c) P3HT:DIBSq:C_{60} planar devices.

The reported exciton diffusion length in C_{60} is 40 nm,[22] while it is only 8 nm in P3HT,[23] suggesting that fewer excitons originating in P3HT are able to reach the dissociating interface. As such, the *IQE* of C_{60} in the binary P3HT:C_{60} device is larger than that of P3HT.

The *IQE* values of DIBSq and C_{60} in the ternary device are significantly lower than those in the DIBSq:C_{60} binary device, which may be attributed to the larger distance that charge carriers have to travel to reach the electrodes, as well as a potentially less favourable charge transfer step at the P3HT:DIBSq interface.

The EPR and EQE results for the P3HT:DIBSq:PCBM and P3HT:DIBSq:C_{60} systems are consistent with the conclusion that the P3HT:DIBSq interface does not dissociate excitons efficiently, despite the apparently large chemical potential (energy offsets). However, as shown by the non-zero EQE spectrum for the ternary planar device, transfer of free charge carriers across the P3HT:DIBSq interface is favourable. Even though the P3HT:DIBSq interface does not dissociate excitons, the relatively high power conversion efficiency, EQE response[4] and the EPR data for P3HT:DIBSq:PCBM BHJ devices, all indicate that exciton dissociation is very efficient in these devices. Energy transfer from P3HT to DIBSq was previously shown to be efficient[4] and appears to be crucial in achieving efficient exciton dissociation. The energy transfer mechanism provides the opportunity for excitons created in P3HT to move to the DIBSq:PCBM interface and consequently dissociate. Such a multistep exciton dissociation process was predicted by the kinetic Monte Carlo modelling.[6] Table I indicates that no contribution of P3HT to the photocurrent was seen in the planar devices under study. The exciton diffusion length in DIBSq is reported to be only 1.6 nm,[19] while the DIBSq layer thickness for our devices was 10 nm. Hence, excitons in the DIBSq layer that are near the P3HT interface are not able to diffuse to the fullerene interface where they can dissociate. The Förster radius for energy transfer from P3HT to DIBSq is approximately 5 nm.[6] Consequently, if the DIBSq thickness is less than 7 nm, a P3HT contribution to the photocurrent may be expected. We fabricated a ternary planar device with a DIBSq

thickness of 6 nm, and indeed a significant P3HT contribution was seen in the EQE spectrum (see supplementary material), which corroborates the previous reports of energy transfer from P3HT to DIBSq. This work demonstrates that energy level information of isolated materials is insufficient to predict whether an interface can facilitate exciton dissociation and that energy transfer relaxes the energy level requirements for optimised, multi-component organic solar cells. The high efficiency of the P3HT:DIBSq:PCBM system therefore appears to be a serendipitous achievement, rather than the result of careful electronic energy level engineering.

See supplementary material for a more detailed explanation of how the P^+ population was calculated, a figure showing the EPR spectra measured at both 170 K and 200 K, a depiction of the planar device structures and associated absorption spectra, the EQE spectrum of a ternary planar device with a DIBSq thickness of 6 nm and, lastly, the real and imaginary components of the dielectric function of P3HT, C_{60} and DIBSq.

The University of Newcastle is gratefully acknowledged for the travel support to conduct the EPR measurements. The Bruker EMXplus EPR system was funded under the Australian Research Council's Linkage Infrastructure, Equipment and Facilities scheme. Dr. Juita is gratefully acknowledged for her assistance in conducting the EPR measurements. The Office of the Prime Minister of Iraq through the Higher Committee for Education Development (HCED) and the Iraqi Ministry of Higher Education and Scientific Research (MoHESR) are acknowledged for the provision of a PhD scholarship (MaM and MT). This work was performed in part at the materials node of the Australian National Fabrication Facility, a company established under the National Collaborative Research Infrastructure Strategy to provide nano and micro-fabrication facilities for the Australian researchers. The Australian Renewable Energy Agency is gratefully acknowledged for the financial support (KF).

[1]C. W. Tang, Appl. Phys. Lett. **48**, 183 (1986).
[2]K. Feron, W. J. Belcher, C. J. Fell, and P. C. Dastoor, Int. J. Mol. Sci. **13**, 17019 (2012).
[3]T. Ameri, P. Khoram, J. Min, and C. J. Brabec, Adv. Mater. **25**, 4245 (2013).
[4]J.-S. Huang, T. Goh, X. Li, M. Y. Sfeir, E. a. Bielinski, S. Tomasulo, M. L. Lee, N. Hazari, and A. D. Taylor, Nat. Photonics **7**, 479 (2013).
[5]G. D. Scholes and G. Rumbles, Nat. Mater. **5**, 683 (2006).
[6]K. Feron, J. M. Cave, M. N. Thameel, C. O'Sullivan, R. Kroon, M. R. Andersson, X. Zhou, C. J. Fell, W. J. Belcher, A. B. Walker, and P. C. Dastoor, ACS Appl. Mater. Interfaces **8**(32), 20928–20937 (2016).
[7]R. A. J. Janssen and J. Nelson, Adv. Mater. **25**, 1847 (2013).
[8]J. D. Servaites, B. M. Savoie, J. B. Brink, T. J. Marks, and M. A. Ratner, Energy Environ. Sci. **5**, 8343 (2012).
[9]R. C. Chiechi, R. W. A. Havenith, J. C. Hummelen, L. J. A. Koster, and M. A. Loi, Mater. Today **16**, 281 (2013).
[10]B. P. Rand, D. P. Burk, and S. R. Forrest, Phys. Rev. B **75**, 115327 (2007).
[11]V. Helenius, R. Monshouwer, and R. van Grondelle, J. Phys. Chem. B **101**, 10554 (1997).
[12]J. D. A. Lin, O. V. Mikhnenko, T. S. van der Poll, G. C. Bazan, and T.-Q. Nguyen, Adv. Mater. **27**, 2528 (2015).
[13]S. Athanasopoulos, E. V. Emelianova, A. B. Walker, and D. Beljonne, Phys. Rev. B **80**, 195209 (2009).
[14]A. Lefrançois, B. Luszczynska, B. Pepin-Donat, C. Lombard, B. Bouthinon, J.-M. Verilhac, M. Gromova, J. Faure-Vincent, S. Pouget, F. Chandezon, S. Sadki, and P. Reiss, Sci. Rep. **5**, 7768 (2015).
[15]M. S. A. Abdou, F. P. Orfino, Y. Son, and S. Holdcroft, J. Am. Chem. Soc. **119**, 4518 (1997).
[16]V. I. Krinichnyi and E. I. Yudanova, AIP Adv. **1**, 22131 (2011).
[17]V. I. Krinichnyi, H.-K. Roth, S. Sensfuss, M. Schrödner, and M. Al-Ibrahim, Phys. E **36**, 98 (2007).
[18]G. Chen, H. Sasabe, T. Igarashi, Z. Hong, and J. Kido, J. Mater. Chem. A **3**, 14517 (2015).
[19]G. Wei, X. Xiao, S. Wang, K. Sun, K. J. Bergemann, M. E. Thompson, and S. R. Forrest, ACS Nano **6**, 972 (2012).
[20]N. C. Nicolaidis, B. S. Routley, J. L. Holdsworth, W. J. Belcher, X. Zhou, and P. C. Dastoor, J. Phys. Chem. C **115**, 7801 (2011).
[21]M. Tian, M. Furuki, I. Iwasa, Y. Sato, L. S. Pu, and S. Tatsuura, J. Phys. Chem. B **106**, 4370 (2002).
[22]P. Peumans, A. Yakimov, and S. R. Forrest, J. Appl. Phys. **93**, 3693 (2003).
[23]P. E. Shaw, A. Ruseckas, and I. D. W. Samuel, Adv. Mater. **20**, 3516 (2008).